Start and stop systems on agricultural tractors as solution for saving fuel and emissions

Start and stop systems on agricultural tractors as solution for saving fuel and emissions

Michele Mattetti[a], Amerigo Beltramin[a], Manuel Antonio Perez Estevez[b] , Massimiliano Varani[a], Massimiliano Renzi[b], Luigi Alberti[c]*

[a] *Department of Agricultural and Food Sciences – Alma Mater Sudiorum - University of Bologna, Bologna, Italy*
[b] *Faculty of Science and Technology, Free University of Bozen/Bolzano, Bozen, Bolzano, Italy*
[c] *Dep. of Industrial Engineering University of Padova, Padova, Italy*

* *Massimiliano Varani, e-mail: massimiliano.varani @unibo.it*

KEYWORDS: idling, green-house emissions, CANBUS, climate change, real-world data

η_{alt}	alternator efficiency	(-)
η_{eng}	diesel engine efficiency	(-)
η_{cha}	battery charging efficiency	(-)
η_{disc}	battery discharging efficiency	(-)
ρ_{CO}	density of CO at the exhaust	(kg m^{-3})
ρ_{CO_2}	density of CO_2 at the exhaust	(kg m^{-3})
ρ_{fuel}	fuel density	(kg m^{-3})
c_{CO}	Carbon monoxide (CO) concentration	(ppm)
c_{CO_2}	Carbon dioxide (CO_2) concentration	(%)
h_{fuel}	fuel lower heating value	(MJ kg^{-1})
$\dot{f}$	Engine fuel rate	(L h^{-1})
$\dot{f}_{idle}$	Engine fuel rate during idling	(L h^{-1})
$f_{el,st}$	amount of burned fuel necessary for restoring $E_{el,st}$ in the battery when the engine is running	(kg)
$f_{inj,st}$	fuel injected to accelerate the engine up to the minimum self-sustaining engine rotational speed	(kg)
f_{save}	potential fuel savings	(L)
$\dot{m}_{CO}$	mass flow of CO	(kg h^{-1})
$\dot{m}_{CO_2}$	mass flow of CO_2	(kg h^{-1})
$m_{CO,el\ st}$	CO emissions for starting the engine	(kg)
$m_{CO_2,el\ st}$	CO_2 emissions for starting the engine	(kg)
$\dot{m}_{CO,idle}$	CO mass flow rate during idling	(kg h^{-1})
$\dot{m}_{CO_2,idle}$	CO_2 mass flow rate during idling	(kg h^{-1})
$m_{CO,inj,st}$	CO emissions generated for accelerating the engine up to the minimum self-sustaining engine rotational speed	(kg)
$m_{CO_2,inj,st}$	CO_2 emissions generated for accelerating the engine up to the minimum self-sustaining engine rotational speed	(kg)
$m_{CO,save}$	potential CO savings	(kg)

$m_{CO_2,save}$	potential CO_2 savings	(kg)
n	Engine rotational speed	(rpm)
n_{ign}	number of additional engine restarts	(-)
n_{PTO}	Rear PTO rotational speed	(rpm)
p	Exhaust gas pressure, equal to the ambient pressure	(Pa)
$t_{eq,idle,f}$	equivalent idling seconds of fuel	(s)
$t_{eq,idle,CO}$	equivalent idling seconds of CO	(s)
t_s	duration of the engine start-up	(s)
t_{unn}	Duration of unnecessary idling	(s)
v_t	Tractor ground speed	(km h^{-1})
$E_{el,st}$	energy required by the starter to run the engine	(J)
E_{ICE}	energy that must be given by the engine to recharge the energy delivered by the battery during the electric start-up	(J)
I_{batt}	Battery Current	(A)
I_{un}	unnecessary idling logical variable	(-)
K_{CO}	CO emission factor assumed to be the maximum allowable according to the limits established in the European emission standards for non-road mobile machinery specified in Stage V regulation	(g kW^{-1} h^{-1})
M_*	molecular weight	(g mol^{-1})
O_p	Presence of the operator on the seat of the vehicle	(-)
P_{batt}	power delivered by the battery	(W)
R	gas constant	(J K^{-1} mol^{-1})
RHP	Position of the rear three-point hitch	(%)
T_c	Engine coolant temperature	(°)
T_{exh}	temperature of the gases at the exhaust	(K)
V_{batt}	Battery Voltage	(V)
$\dot{V}_{CO}$	volume rate of CO	(m^3 h^{-1})
$\dot{V}_{CO_2}$	volume rate of CO_2	(m^3 h^{-1})
$\dot{V}_f$	Volume rate of fuel gasses	(m^3 h^{-1})
$\dot{V}_{fi}$	Oil flow through the auxiliary valve in percentage with respect to the maximum flow. i stands for the number of the auxiliary valves (i.e., 0, 1, 2, and 3)	(L min^{-1})

Abstract

Agricultural tractors may idle from 10 to 43% of their entire operating life and this inoperative time must be minimised because it is detrimental to the environment, public health, fuel economy, and engine lifespan (Perozzi et al., 2016). On passenger cars, start and stop (SS) systems have been extensively used, but they are not currently installed in any

commercial tractor. Studies show that for very short idling stops SS systems might be ineffective for the additional energy required for re-starting the engine. This study aims to investigate the potential advantages of SS systems on agricultural tractors. To this aim, the energy required for engine start-up and the subsequent emissions were measured and then compared with the energy and the emissions during idling. Moreover, a predefined control strategy of the SS system was developed, and its potential fuel and emission savings were estimated using real-world data. In terms of fuel consumption and CO emission, turning off the engine is recommended for stops longer than 4 s and 134 s, respectively. From the collected real-world data, the tractor was run on idle for 21.7% of the entire operating duration. The results obtained with the SS control strategy developed in this paper applied to the US area, where there are 1.2 million tractors of the same power level of the tractor used in this study with a yearly usage up to 850 h, would permit to save 285.6 million litres of fuel, and, respectively of 16.5 and 754 tons of CO and CO_2.

Introduction

The agricultural sector is responsible for about 21% of the world's greenhouse gas emissions, mainly due to the use of fossil-based fertilisers, the combustion of biomass and the polluting gas emissions of agricultural machinery (Qiao et al., 2019). Most of the self-propelled agricultural machinery are powered by endothermic engines, where fossil fuels still represent 95% of the forms of energy used for their propulsion (IPPC, 2014). Nearly all modern agricultural tractors are propelled by diesel engines, so during fuel combustion process, polluting gases such as carbon monoxide (CO), nitrogen oxides (NO_X), particulate matter (PM), and hydrocarbons (HC) are emitted together with greenhouse gases, like CO_2. These gases are strictly regulated by emission Stages (or Tiers) introduced by European and US legislators. To comply with these emission limits, present-day tractors are equipped with several emission reduction technologies such as Diesel Particulate Filter (DPF), Exhaust Gases Recirculation (EGR), Diesel Oxidation Catalyst (DOC) and Selective Catalytic Reduction (SCR) (Rudder, 2012). A further solution to reduce the emission of polluting gases is to reduce the time spent by the tractor in idle condition. Vehicles idling time could be classified in two main categories: necessary or unnecessary (Brodrick, Lipman, et al., 2002). While the former cannot be eliminated since it is needed for the vehicle operation (e.g., engine heating during start-up), the latter may occur for the negligence of drivers. Unnecessary idling is frequent for road trucks due to driver mandatory rest periods, where drivers keep the engine idling to maintain the battery voltage and the cab temperature at their optimal levels. In the USA, on average, long-haul trucks idle for about 1800 hours per year consuming more than 5500 litres of diesel (Argonne National Laboratory, 2015). Even agricultural tractors are exposed to prolonged idling periods; indeed, an extended field campaign on a fleet of tractors showed that tractors idle for a period that ranges from 10% to 43% of the time (Perozzi et al., 2016). Molari et al. (2019) investigated the reasons for idling

by monitoring the activity of an agricultural tractor through a dashcam and a CANBUS data logger. Results show that about 67% of the idling stops were mainly due to the driver's behaviour (i.e., talk among drivers, use of the mobile phone, etc.) while the remaining 33% of time required the use of any subsystem of the tractor, such as the hydraulic pump necessary for implement hitching and servicing. During idling, the fuel efficiency of internal combustion engines drops of 20% with respect to nominal operating conditions (Brodrick et al., 2002a) and in this condition, the fuel is mostly used to run accessories and auxiliaries that, on heavy duty vehicles (i.e., trucks, and agricultural tractors), are mechanically driven leading to parasitic loadings (Saetti et al., 2021). The necessary idling could be reduced with tractor subsystems electrification, however the high investment costs to develop this technology still hinder its use (Scolaro et al., Submitted). On the other hand, unnecessary idling could be simply reduced with the adoption of start-stop (SS) systems, which represents a low-cost hybridisation technology widely spread among modern automotive vehicles (Salmasi, 2007). These devices are controlled by the engine control unit (ECU) and its duty is to automatically shut-off the engine when it starts idling. Bench tests performed on different cars and with different test cycles demonstrated that improvement in fuel efficiency thanks to SS could vary from 1% to 14.4 % (Wishart et al., 2012). In real world conditions, the improvement in the fuel efficiency due to SS is even more variable for the several intercorrelated variables (i.e., itineraries, traffic loads, weather conditions, and driver behaviour) that affect the duration and the number of idling stops (Abas et al., 2017; Thitipatanapong et al., 2013). A key factor for an efficient SS system is a well-designed and smart control algorithm that is able to avoid the engine shut-off for very short idling periods. Indeed, the engine restarts require additional energy and, to obtain an overall positive effect, this energy must be lower than the energy consumed by the engine idling. Tests performed on a medium size car demonstrated that SS systems are convenient only when idling stops are longer than 10 s (Gaines et al., 2013). At

present, to the authors' knowledge, no significant studies on the implementation of SS systems specifically designed for agricultural tractors are available in literature. The aim of this work is to evaluate the energy demand and the pollutant gas emissions of a tractor diesel engine during the start-up and idling phase in order to evaluate the potential benefits of an SS system in this type of tractors. In addition, the proper timings and strategies to adopt SS are discussed in order to achieve advantages in terms of reducing fuel consumption, carbon dioxide and carbon monoxide emissions.

Materials and methods

Data acquisition

The tractor used for the test was a New Holland T7.260 PowerComamand^{tm} (CNH Industrial N.V., Amsterdam, Netherlands) whose specifications are reported in Table 1. This type of tractor was chosen since tractors of this class are rich in embedded sensors allowing comprehensive monitoring of the activity of the different embedded subsystems.

Table 1 – Specifications of the tractor used for the test

Engine type	Turbo Diesel
Number of cylinders	6
Engine displacement [cm^3]	6700
Engine tier (emission reduction technologies)	4A (DOC, DPF, SCR)
Nominal power [kW]	162 at 2200 rpm
Torque [Nm]	1000 at 1500 rpm
Unladen mass [kg]	8140
12V alternator [A]	150
Battery capacity [Ah]	176
Battery cold cranking ability [CCA]	1300

Two types of tests were carried out:

- **Engine start test**: for measuring the energy necessary for starting the engine and the correlated emissions;

- **Real world test:** for evaluating the potential fuel and emissions savings in using a SS system with a specified control strategy.

Engine start test

Test description

For this test, the NI CompactDAQ 9178 (National Instruments, Austin, TX, USA) equipped with a NI 9215 (National Instruments, Austin, TX, USA) as analogue input and a NI 9861 (National Instruments, Austin, TX, USA) as CANBUS input was used. The NI 9215 was connected with:

- battery poles for measuring the voltage at the battery (V_{batt}).
- current transducer HAT 500–S (LEM Holding, Plan-les-Ouates, Switzerland) installed on the negative pole of the battery, to record the current flow towards the battery (I_{batt}). This value was positive in case the current flows to the battery and negative otherwise.

The NI 9215 was set up to sample data at 1000 Hz, this frequency was chosen after preliminary tests, where it was demonstrated to be fast enough to properly record current and voltage peaks during the ignition process. The NI 9861 was set up to record the CANBUS signals with the following specified Suspect Parameter Numbers (SPNs) and Parameter Group Numbers (PGNs):

- SPN 190 and PGN 61444, *"Engine speed"* reporting the revolution speed of the engine crankshaft, denoted as "n" in the following. Sampling rate = 10 Hz.
- SPN 183 and PGN 65266, *"Engine fuel rate"* reporting the litres of fuel consumed by the engine per hour of running. This value is denoted as *"$\dot{f}$"* in the following. Sampling rate = 10 Hz.

- SPN 110 and PGN 65262, "*Engine coolant temperature*" reporting the temperature of the liquid found in the engine cooling system. The value is denoted as *"T_c"* in the following. Sampling rate = 1 Hz.

Moreover, at the exhaust, the gas analyser MRU Vario Plus Industrial (MRU air fair emission monitoring systems, Humble, TX, USA) was installed in order to measure the concentration of pollutants at the vehicle exhaust pipe. The concentration for carbon dioxide (CO_2) and carbon monoxide (CO) are denoted as c_{CO_2} and c_{CO}, respectively. The instrument also recorded the temperature of the fuel gases at the exhaust (T_{exh}). All the data recorded from the gas analyser were sampled at 0.5 Hz. This instrument complies with US-EPA methods CTM-030 (US EPA, 1997) and CTM-034 (US EPA, 1999) and international ASTM D6522 (ASTM International, 2011); it has been certified according to DIN EN 50379-1 (BSI Standards, 2012a) and DIN EN 50379-2 (BSI Standards, 2012b). The gas analyser is also able to measure the nitrogen oxides (NO_x); however, they were not analysed in detail in this work since this study is focused on the engine idling and in this condition, the combustion temperature is low and so the NO_x concentration. Indeed, Nada et al show the exponential relationship between NOx and temperature (Nada et al., 2015). The test procedure consisted of 10 cycles composed of 60 s of engine idling, and 30 s of engine off (Fig. 1).

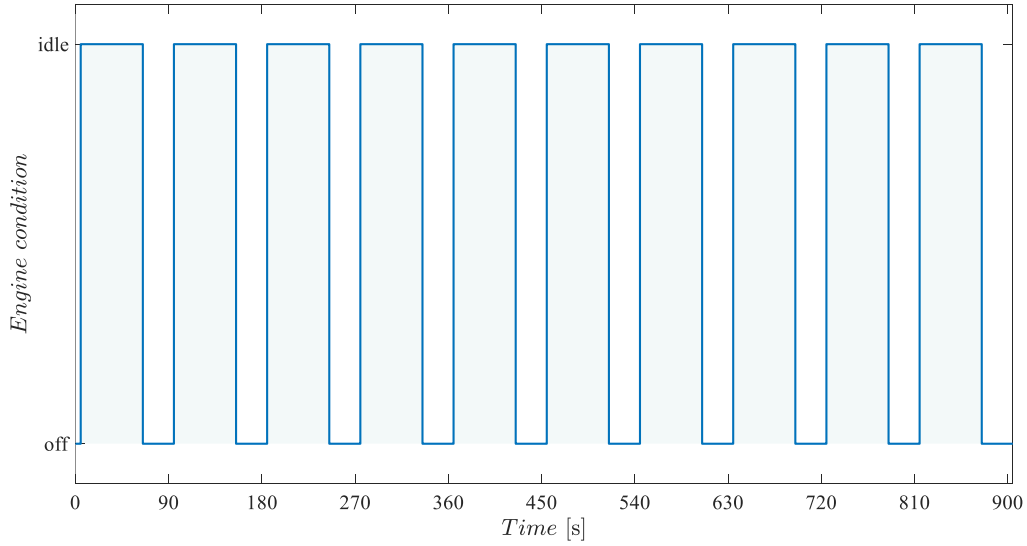

Fig. 1- Engine duty-cycle of the engine start tests. Each ignition is followed by 60 seconds of idle and then 30 seconds of stop.

The idling duration was chosen in order to maintain V_{batt} at the voltage level prior engine starting, as shown in Fig.2. This condition was chosen as SS systems do not work when the state of charge of the battery is not at the optimal level. The cycles were carried out with the auxiliaries active (denoted AUX ON in the following) and inactive (denoted AUX OFF in the following). The considered auxiliaries were the lights (front and rear headlights, work lamps, warning beacon), the cab radio, the heating, ventilation and air conditioning (HVAC) compressor, and the blower fan, which was set at its maximum speed. All the auxiliaries except for the HVAC compressor are powered by the battery leading to an electrical loading. When the engine was off, the auxiliaries were left on as usually occurs with vehicles equipped with SS systems. All the tests were conducted at the optimal engine working temperature condition ($T_c \approx 79\,°C$ according to the tractor manufacturer recommendation) as SS systems do not work if the engine temperature is too low due to the greater friction losses and gaseous emissions when the engine is cold (Hadavi et al., 2013; Lee et al., 2019). Thus, prior to the test, the engine was left idling until reaching the optimal T_c.

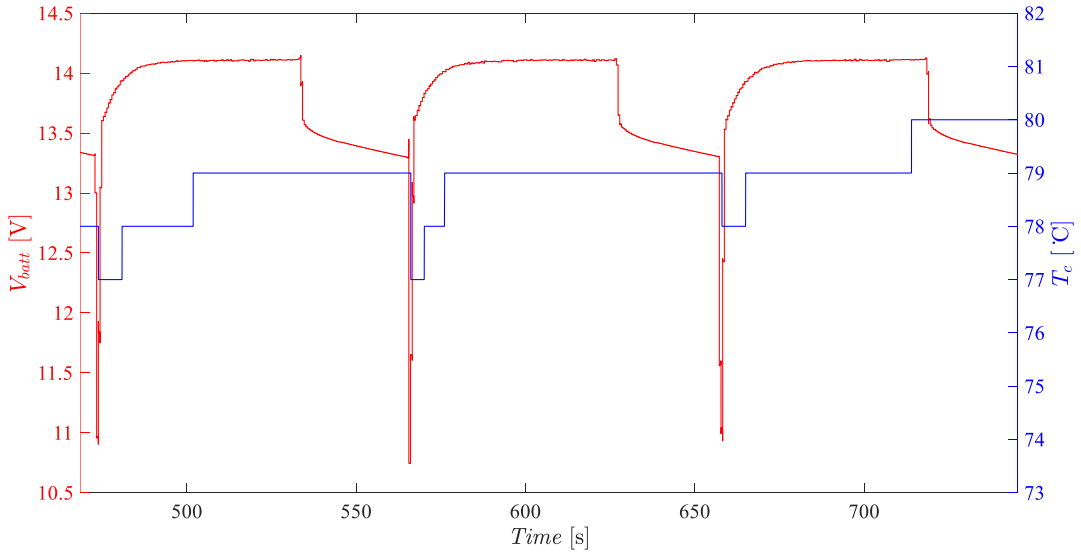

Fig. 2 – Portion of battery voltage signal (V_{batt}) (red) and engine coolant temperature (T_c) behaviour (blue) during the test in the AUX OFF condition.

All the acquired signals were resampled at 1000 Hz using a cubic spline interpolation for a consistent sampling rate among the recorded signals. From the recorded signals, the electric power delivered by the battery (P_{batt}) was calculated with equation 1:

$$P_{batt}=V_{batt}I_{batt} \quad (1)$$

In order to be able to compare the emissions measurements with the electrical and ICE measurements, the delay of the emissions measurements was removed by subtracting the average time difference between the fuel injection peaks (enclosed in the blue markers in Fig. 3) and the emissions peaks (enclosed in the green markers in Fig. 3). This delay is due to the time constant of the sensors, the time taken for the combustion process to occur, and the time taken by the combustion gases to reach the exhaust after fuel injection; the latter two are considerably smaller than the first one. The c_{CO_2} and c_{CO} delay is shown in Fig. 3, together with the shifted curves.

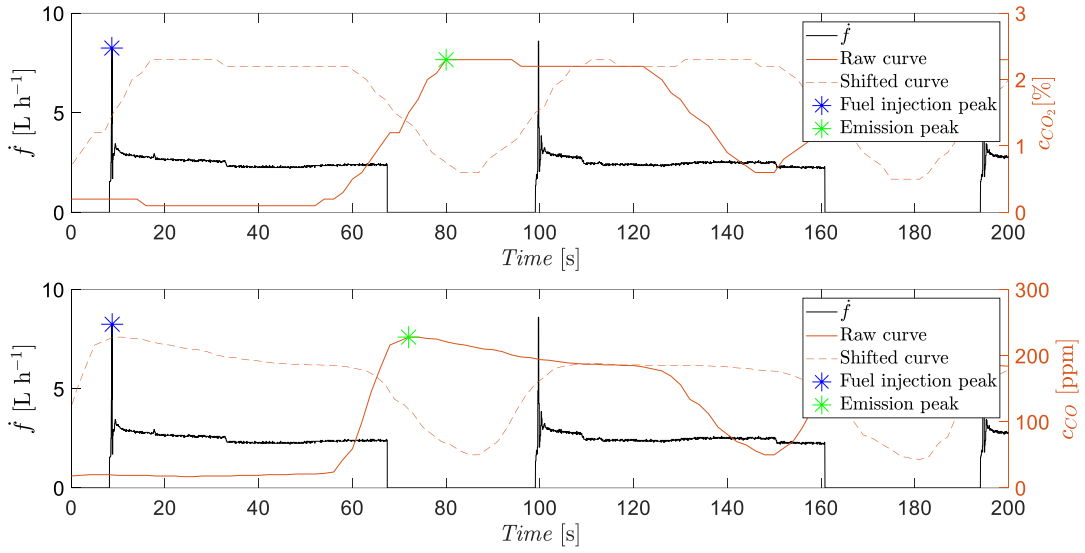

Fig. 3 – Portion of fuel rate ($\dot{f}$), CO concentration (c_{CO}) and CO2 concentration (c_{CO_2}) for showing the removal of the delay of the emissions curves. The blue markers corresponds to fuel injection peaks; while the green markers, highlight emissions peaks.

With the aim of better analysing the emissions, the relative measurements of volumetric concentration obtained with the gas analyser have been converted to absolute quantities using the fuel consumption registered by the CANBUS. The procedure used for this conversion is reported below. Diesel fuel is a mixture of hydrocarbons, mainly paraffins, but its exact composition varies depending on the supplier, the final application and the period of the year. In this case, it was hypothesised that the average chemical composition of the used fuel was $C_{12}H_{23}$. Using the oxidation reaction and assuming complete combustion, which is a good approximation for this type of calculation in diesel engines where the amount of air is considerably higher than the stoichiometric one, it can be found that for each litre of fuel burned approximately 2.624 kg of CO_2 are produced (Geerlings & van Duin, 2011). Thus, the mass flow of CO_2 emissions was calculated using equation 2:

$$\dot{m}_{CO_2} = 2.624\,\dot{f} \qquad (2)$$

To estimate the mass flow of CO, the following procedure was adopted:

a) The volume rate of CO_2 ($\dot{V}_{CO_2}$) was calculated using equation 3. The density of CO_2 at the exhaust (ρ_{CO_2}), for each time step, was estimated using the ideal gas equation (equation 4).

$$\dot{V}_{CO_2} = \frac{\dot{m}_{CO_2}}{\rho_{CO_2}} \quad (3)$$

$$\rho_* = \frac{p\ M_*}{R\ T_{exh}} \quad (4)$$

where:

- ρ_* is the density of CO and CO_2 (namely, ρ_{CO} and ρ_{CO_2});
- p is the gas pressure equal to the ambient pressure (i.e., 101.325 kPa);
- M_* is the molecular weight, equal to 44 g mol^{-1} for CO_2 and 28 g mol^{-1} for CO;
- R is the gas constant, equal to 8.314 J K^{-1} mol^{-1}.

b) The volume rate of fuel gases ($\dot{V}_f$) and CO ($\dot{V}_{CO}$) were estimated using c_{CO_2} and c_{CO} with equations 5 and 6, respectively.

$$\dot{V}_f = \dot{V}_{CO_2} / c_{CO_2} \quad (5)$$

$$\dot{V}_{CO} = \dot{V}_f\ c_{CO}\ 10^{-6} \quad (6)$$

c) The mass flow of CO ($\dot{m}_{CO}$) was calculated with equation 7, while the density of CO at the exhaust (ρ_{CO}) was calculated using the ideal gas law reported in equation 4.

$$\dot{m}_{CO} = \rho_{CO}\dot{V}_{CO} \quad (7)$$

For each starting cycle, signals were divided into two parts, one related to the engine start-up and the other related to the engine idling. This allowed to quantify the fuel and the pollutant masses required for both parts. The first part can in turns be subdivided in two:

- **electric start:** corresponding to the electrical energy demanded by the starter to run the engine. This was absorbed by the starter from the battery in the time frame between the instants $t_1$and t_2. This time frame was detected by selecting the portions of the signals where the P_{batt} was greater than a given threshold (i.e., -0.9 kW and -0.1 kW for AUX ON and AUX OFF, respectively) defined by observing the value of P_{batt} when the engine was off (Fig. 4).
- **fuel injection:** corresponding to the period in which fuel is injected for accelerating the engine from 0 rpm up to the minimum self-sustaining engine rotational speed (i.e., 840 rpm). It is delimited by the instants t_3 and t_4 (Fig. 4). The former was defined by observing when $\dot{f}$ started to be greater than 0 L h^{-1}, while the latter when n started to be greater than 840 rpm.

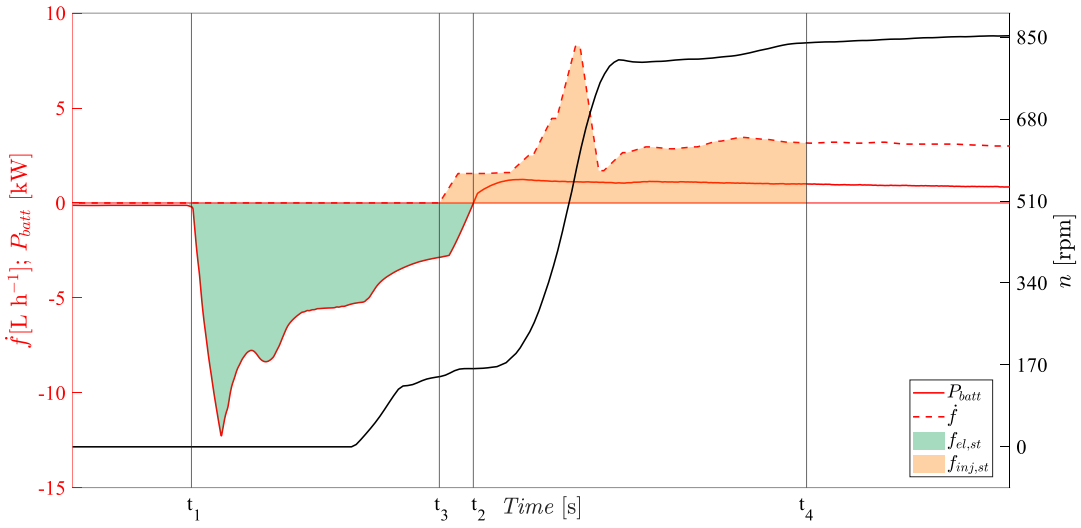

Fig. 4 – Portion of fuel rate ($\dot{f}$), battery power (P_{batt}), and engine speed (n) during a single ignition (AUX OFF). The green area reports the energy required by the starter to run the engine ($E_{el,st}$), while in orange the amount of fuel injected to bring the engine to the self-sustaining speed ($f_{inj,st}$).

The **idling** part was identified as the portion in which the n was between 840 rpm and 860 rpm and its portion is delimited by the instants t_4 and t_5 (Fig. 5). In this period, the fuel was used to sustain the engine and eventually the auxiliaries.

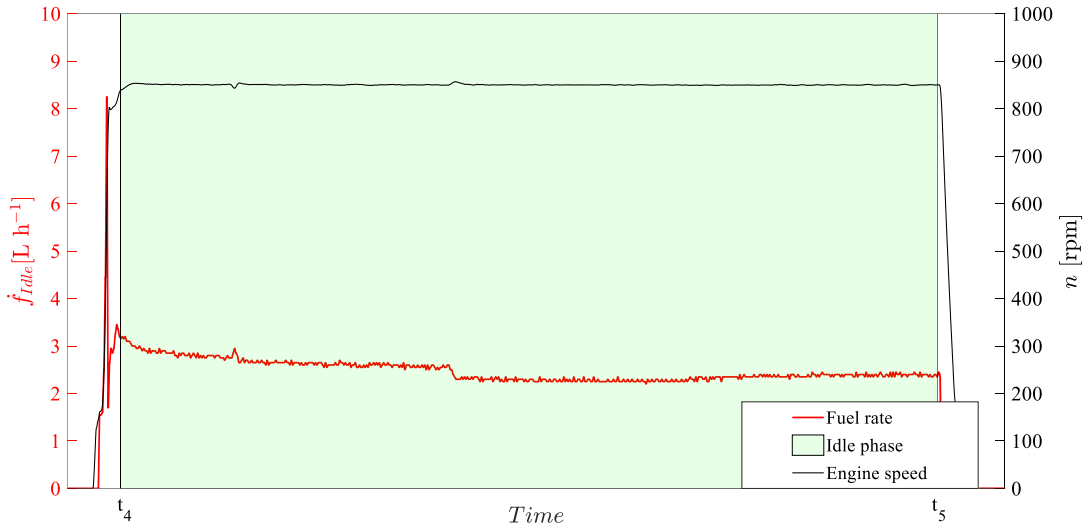

Fig. 5- Portion of fuel rate ($\dot{f}$) and engine speed (n) during a cycle. The portion highlighted in green underlines the idling part of the cycle.

After having classified the signal portions in the start-up event, the following metrics were calculated:

- the duration of the start-up (t_s) with equation 8.

$$t_s = t_4 - t_1 \tag{8}$$

- energy demanded by the starter to start the engine ($E_{el,st}$) with equation 9:

$$E_{el,st} = \int_{t_1}^{t_2} P_{batt} dt \tag{9}$$

- amount of burned fuel necessary for restoring $E_{el,st}$ in the battery when the engine is running ($f_{el,st}$) using equation 10:

$$f_{el,st} = \frac{E_{el,st}}{(\eta_{disc}\eta_{cha}\eta_{eng}\eta_{alt}) * (h_{fuel}\rho_{fuel})} \tag{10}$$

where:

  - η_{disc}, battery discharging efficiency set to 0.85 (Ganesan & Sundaram, 2012);

241 ○ η_{cha}, battery charging efficiency set to 0.85 (Kulikov & Karpukhin, 2018);

242 ○ η_{eng}, diesel engine efficiency set to 0.45 (Patton & Bennett, 2011);

243 ○ η_{alt}, alternator efficiency set to 0.6 according to Saetti et al. (2021);

244 ○ ρ_{fuel}, fuel density, set to 827 $kg\ m^{-3}$ (Parravicini et al., 2020);

245 ○ h_{fuel}, fuel lower heating value, set to 43.51 $MJ\ kg^{-1}$ (Parravicini et al., 2020).

246 • greenhouse emissions for starting the engine ($m_{CO_2,st}$) using equation (11).

$$m_{CO_2,st} = 2.624\ f_{el,st} \quad (11)$$

247 • CO emissions for starting the engine ($m_{CO,el\ st}$) using equations 12 and 13:

$$E_{ICE} = \frac{E_{el,st}}{(\eta_{disc}\eta_{cha}\eta_{alt})} \quad (12)$$

$$m_{CO,el\ st} = K_{CO}E_{ICE} \quad (13)$$

248 where:

249 ○ E_{ICE}: energy that must be given by the engine to recharge the energy delivered
250 by the battery during the electric start-up.

251 ○ K_{CO}: CO emission factor assumed to be the maximum allowable according to
252 the limits established in the European emission standards for non-road mobile
253 machinery specified in Stage V regulation (3.5 g kW^{-1} h^{-1}) (International
254 Council on Clean Transportation, 2016). This was carried out in order to
255 establish a general condition for CO emissions during the battery charging
256 process. In reality, this value changes depending on the use of the tractor after
257 ignition that determines the engine load. The value might be lower than that
258 reported here leading to conservative results.

- the fuel injected to accelerate the engine up to the minimum self-sustaining engine rotational speed ($f_{inj,st}$) using equation 14.

$$f_{inj,st} = \int_{t_3}^{t_4} \dot{f}\, dt \tag{14}$$

- CO_2 and CO emissions generated for accelerating the engine up to the minimum self-sustaining engine rotational speed (respectively, $m_{CO_2,inj,st}$ and $m_{CO,inj,st}$) using equations 15 and 16, respectively:

$$m_{CO_2,inj,st} = 2.624\ f_{inj,st} \tag{15}$$

$$m_{CO,inj,st} = \int_{t3}^{t4} \dot{m}_{CO}\, dt \tag{16}$$

- idling fuel consumption ($\dot{f}_{idle}$) corresponding to the average value of $\dot{f}$ during the time frame t_4 and t_5.
- The CO_2 mass flow rate during idling ($\dot{m}_{CO_2,idle}$) was calculated using equation 17, which is derived from equation 2 with $\dot{f}_{idle}$ instead of $\dot{f}$:

$$\dot{m}_{CO_2,idle} = 2.624\ \dot{f}_{idle} \tag{17}$$

- The CO in idling conditions ($\dot{m}_{CO,idle}$) was estimated with eq. 6 as the average of $\dot{m}_{CO}$ during the corresponding period; specifically, from t_4 to t_5.

The sum between $f_{el,st}$ and $f_{ign,st}$, and the sum between $m_{CO,el\ st}$ and $m_{CO,inj\ st}$ are the total fuel consumed and the total CO pollutant emission for an engine restart, respectively. Both permit to calculate the duration of idling that lead to the same energy expenditure ($t_{eq,idle,f}$) and CO emission ($t_{eq,idle,CO}$) of an engine restart and they were calculated with equations 18 and 19, respectively:

$$t_{eq,idle,f} = \frac{\left(f_{el,st} + f_{inj,st}\right)}{\dot{f}_{idle}} \quad (18)$$

$$t_{eq,idle,CO} = \frac{\left(m_{CO,inj,st} + m_{CO,el,st}\right)}{\dot{m}_{CO,idle}} \quad (19)$$

In other words, $t_{eq,idle,*}$ provides the number of seconds of idling beyond which shutting down the engine could bring benefits in terms of consumed fuel or in terms of CO emissions.

Real world test

The tractor used for the engine start test was monitored for three years and it accumulated 1314 hours of use. In particular, a CANBUS data logger was installed on the tractor, as already discussed by the Authors in other studies (Mattetti et al., 2021; Molari et al., 2013). For the analysis, in addition to the CANBUS signals recorded during the engine start tests, the CANBUS signals with the following SPNs and PGNs were considered:

- SPNs: 1907, 1919, 1931, 1943 and PGNs 65072, 65073, 65074, 65075, "*Auxiliary valve number port flow*" reporting the flow through the valve in percentage with respect to the maximum flow. These signals are denoted as $\dot{V}_{fi}$ in the following, where i stands for the number of the auxiliary valves (i.e., 0, 1, 2, and 3). Sampling rate = 10 Hz
- SPN 9711 and PGN 64388, *"Operator Presence State"* reporting the presence of the operator on the seat of the vehicle. The signal is denoted as O_p in the following, which is equal to 0 when the operator was not on the seat and 1 otherwise. Sampling rate = 10 Hz
- SPN 1873 and PGN 65093, "*Rear hitch position*" reporting the position of the rear three-point hitch in percentage. The signal is 0 when the rear three-point hitch is fully

down and 100% when it is fully up. The signal is denoted as RHP in the following. Sampling rate = 10 Hz

- SPN 1883 and PGN 65090, *"Rear PTO Output Shaft Speed"* reporting the speed of the rear PTO output shaft. The signal is denoted as n_{PTO} in the following. Sampling rate = 10 Hz

In addition to these signals, the machine position and its ground speed (v_t) were measured through the GNSS (Global Navigation Satellite System) receiver embedded into the CANBUS data logger. Through MathWorks MATLAB (Natick, MA, USA), all the signals were imported and interpolated at 10 Hz using a cubic spline so that the sampling rate of all the signals was the same. Idling stops were identified when:

- n lower than 850 rpm;
- v_t equal to 0 km h^{-1};
- n_{PTO} equal to 0 rpm;

Idling stops were classified as unnecessary if they can be avoided with no significant impact on productivity and as necessary otherwise. According to this definition, unnecessary idling occurred anytime the operator did not use the three-point linkage and any auxiliary valves. Thus, an idling stop was classified as unnecessary according to the following rule:

- O_p was 0 for longer than 10 s, chosen on the basis of the results of the engine start test and because very short idling may occur for inadvertent driver manoeuvres;
- the peak-to-peak value of RHP and $\dot{V}_{fi}$ in the idling stop was 0;
- T_c was above 78 °C.

The unnecessary idling was reported with a logical variable denoted as I_{un}, which was 1 when unnecessary idling occurred and 0 otherwise. In Fig.6, an example of classification of both types of idling stops are reported.

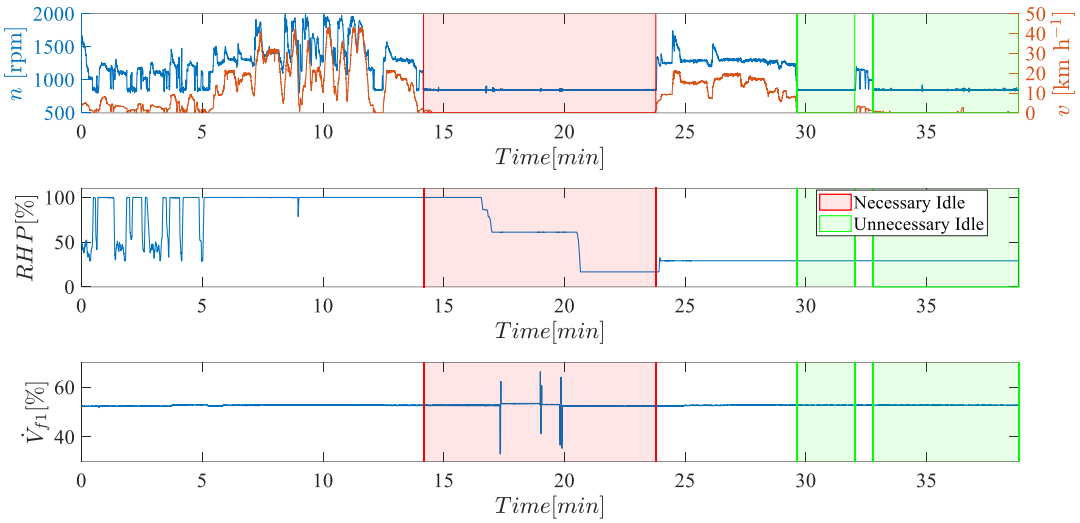

Fig. 6– Example of the idling classification. On top, engine speed (n) and vehicle ground speed (v_t); on the middle, rear hitch position (RHP); on bottom, flow rate of auxiliary valve n. 1 ($\dot{V}_{f1}$). Areas of unnecessary idle are shaded in green, while the area of necessary idling are shaded in red. In the necessary idling stops, the tractor was an idle condition and neither the three-point linkage nor the hydraulic distributors were in use. The $\dot{V}_{f2}, \dot{V}_{f3}, \dot{V}_{f4}$ were 0 %, thus they were not plot for sake of clarity

A SS system would permit to save the fuel waste caused by unnecessary idling, but additional fuel would be used for the greater number of engine restarts. The potential savings of fuel, CO_2, and CO due to the introduction of an SS system are, respectively, denoted as f_{save}, $m_{CO_2,save}$, and $m_{CO,save}$ and they were calculated using equations 20, 21 and 22, respectively.

$$f_{save} = t_{unn}\dot{f}_{idle} - n_{ign}(f_{el,st} + f_{inj,st}) \quad (20)$$

$$m_{CO_2,save} = 2.624\ f_{save} \quad (21)$$

$$m_{CO,save} = t_{unn}\ \dot{m}_{CO,idle} - n_{ign}\left(m_{CO,el\,st} + m_{CO,inj\,st}\right) \quad (22)$$

Where:

- t_{unn} is the duration of unnecessary idling;

- n_{ign} is the number of additional engine restarts counting the number of falling edges of I_{un};

$\dot{f}_{idle}$, $f_{el,st}$, $f_{inj,st}$, $m_{el,st}$, $m_{inj,st}$, and $\dot{m}_{CO,idle}$ used in equation 20 are the average value of the data calculated in the engine start test with AUX ON since it provides the more conservative results.

Results and discussion

Start-ups tests

The typical behaviour of $\dot{f}$ and P_{batt} during an idling cycle are reported in Fig. 7 for AUX ON and OFF tests. For both tests, the signals are characterised by a certain amount of irregularity caused by a few auxiliaries that occasionally demand energy from the engine. Those auxiliaries may be the HVAC (its influence can be observed only for the AUX ON tests), and the brake air compressor (its influence can be observed for both tests and it is automatically engaged when the pressure in the circuit reservoir is below a certain value; thus it could not be controlled during the test) due to their cyclic ON-OFF control logic (Saetti et al., 2021). When the engine is off, P_{batt} is negative since the lights and the cab radio demanded energy from the battery. During the idling phase, $\dot{f}$ decays with a similar trend of the P_{batt} due to the fact that the power demand of the alternator depends on the voltage difference between the alternator and the battery, which decreases with the increase of the battery state of charge (Saetti et al., 2021). Moreover, for the AUX OFF, the decay of P_{batt} during charging is more pronounced than with the AUX ON due to the lower electrical loading.

In other words, with the AUX OFF there is lower energy consumption and most of the power generated by the alternator can be given almost exclusively to the battery. Thus, the

battery state of charge deprived before the start-up is restored in a quicker way than the AUX OFF case.

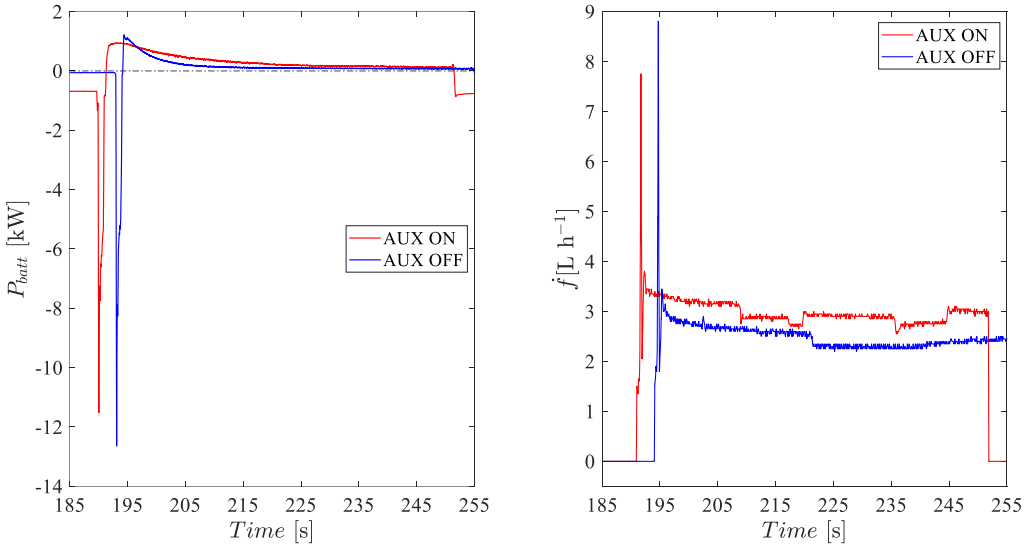

Fig. 7 – Portion of battery power (P_{batt}) and fuel rate ($\dot{f}$) during a cycle for AUX ON and AUX OFF tests. The AUX OFF electric power signals decay to zero faster than the AUX ON signal.

The CO_2 and CO volumetric concentrations in the exhaust registered during the tests are shown in Fig. 8. As expected, the emissions are higher for the AUX ON case, since the electric power demand of the auxiliaries has to be provided by the ICE through the alternator; so, the air fuel mixture should be richer to guarantee the higher required engine power (the idling rotational speed is the same).

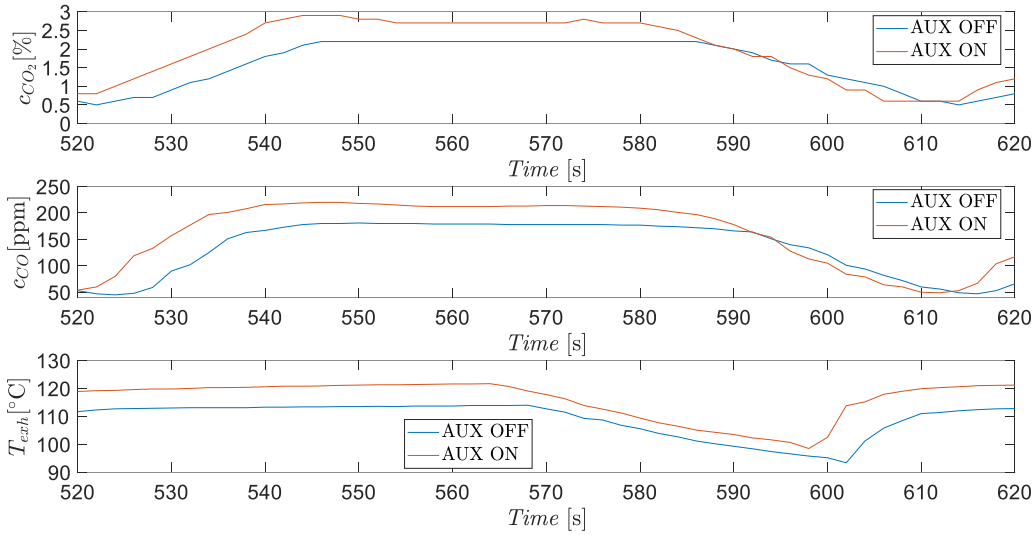

Fig. 8 – Portion of CO_2 concentration (c_{CO_2}), CO concentration (c_{CO}), and exhaust temperature (T_{exh}) during a cycle for AUX ON and AUX OFF tests.

The t_s registered with the AUX ON was 3.10 s (standard deviation= 2.90 10^{-1} s), while the one registered with the AUX OFF was 2.89 s (standard deviation= 2.22 10^{-1} s). t_s is slightly longer with AUX ON because of the engagement of the HVAC compressor leading to greater mechanical loading.

Start-ups tests – fuel consumption metrics

In Table 2, the average values of fuel consumption metrics calculated from the engine start test are reported:

Table 2 - Idle influence on fuel consumption. In the brackets, the standard deviation of each parameter is reported

	AUX OFF	**AUX ON**
$\dot{f}_{Idle}$ [L h^{-1}]	2.40 (6.15 10^{-2})	2.98 (2.69 10^{-2})
$f_{el,st}$ [L]	9.17 10^{-4} (5.87 10^{-5})	1.06 10^{-3} (8.27 10^{-5})
$f_{inj,st}$ [L]	1.39 10^{-3} (5.87 10^{-5})	1.56 10^{-3} (8.54 10^{-5})
$t_{eq,idle,f}$ [s]	3.48 (1.34 10^{-1})	3.16 (1.36 10^{-1})

$\dot{f}_{idle}$ with AUX ON is 24% greater than that with AUX OFF due to the richer air-fuel mixture. This value is significantly lower than that of the heavy duty trucks, probably due to the smaller auxiliaries in tractors than in heavy duty truck (Brodrick, Dwyer, et al., 2002). The greater $\dot{f}_{idle}$ with AUX ON is caused by the greater mechanical and electrical loading caused by the auxiliaries, quantified in the amount of 650 W (standard deviation: 2.44 W). Moreover, for AUX ON, a greater standard deviation value than that with AUX OFF was observed, caused by the higher variability in $\dot{f}$ due to the occasional engagement of some auxiliaries. On average, $t_{eq,idle,f}$ is below 3.5 s in both testing conditions but the greatest calculated value was 3.73 s. Instead, in another study on passenger cars, this quantity was about 10 s (Gaines et al., 2013). This means that for agricultural tractors, the proportion between the energy spent for engine start-up and the idling fuel consumption is different from that for passenger cars. This can be explained by the fact that the tractor used for the tests is equipped with a different engine type (diesel rather than gasoline) and a greater engine size, 6700 cm^3 with respect to the less than 2500 cm^3 of those of the cars used in the above-mentioned study, which leads to a much greater idling fuel consumption (Rakha et al., 2011).

Start-ups tests – emissions metrics

In Table 3, the average values of emission metrics calculated from the engine start test are reported:

Table 3 - Idle influence on emissions. In the brackets, the standard deviation of each parameter is reported

	AUX OFF	**AUX ON**
$\dot{m}_{CO_2,idle}$[kg h^{-1}]	6.29 (6.15 10^{-2})	7.83 (2.69 10^{-2})
$\dot{m}_{CO,idle}$[g h^{-1}]	3.42 10^{-1} (2.25 10^{-2})	3.86 10^{-1} (6.09 10^{-3})
$m_{CO_2 el,st}$ [g]	2.4 (1.55 10^{-1})	2.80 (2.18 10^{-1})
$m_{CO_2 inj,st}$ [g]	3.67 (1.21 10^{-1})	4.11 (2.26 10^{-1})
$m_{CO,el\ st}$ [g]	1.12 10^{-2} (1.00 10^{-3})	1.40 10^{-2} (1.71 10^{-3})
$m_{CO,inj\ ,st}$ [g]	2.78 10^{-4} (4.34 10^{-5})	2.19 10^{-4} (1.15 10^{-5})
$t_{eq,idle,CO}$ [s]	120 (13.3)	134 (15.1)

Since $\dot{m}_{CO_2}$ is proportional to $\dot{f}$ (see equation 2), the same conclusions derived for the metrics related to the fuel flow rate can also be used for the CO_2 related metrics. $m_{CO,el\ st}$ is considerably higher than $m_{CO,inj\ st}$; this could be due to the conversion factor used in this study during the battery charging in the electric start calculation. Specifically, CO emissions were assumed to be the maximum permissible threshold given by the Tier V regulations (3.5 g kW^{-1} h^{-1}). This value might be high but it leads to conservative numbers on the benefits of SS system. $t_{eq,idle,CO}$ is much greater than $t_{eq,idle,f}$ in both testing conditions; thus turning off the engine using a fuel based logic only leads to fuel savings, but might not lead to a reduction of CO emissions, but rather to their increase if the off period is not long enough. On the other hand, a SS configured with a logic based on $t_{eq,idle,CO}$ will have reduced fuel savings as compared to the actual reduction potential. This is due to the high CO emissions of

414 diesel engines at low loads and the lower efficiency of the oxidiser converter at low
415 temperatures.
416
417 *Real-World tests*
418 The tractor was run on idle 21.7% of the entire operating duration, this value is aligned
419 with the average value reported in previous studies (Perozzi et al., 2016). Unnecessary idling
420 accounts for 45% of the total idling time, highlighting the potential advantages of adopting SS
421 systems in agricultural tractors. Idling stops were binned into time intervals as some of the
422 authors carried out in a previous study (Perozzi et al., 2016) and its distribution and their
423 contribution to the idling duration are reported in Figure 9 (top).

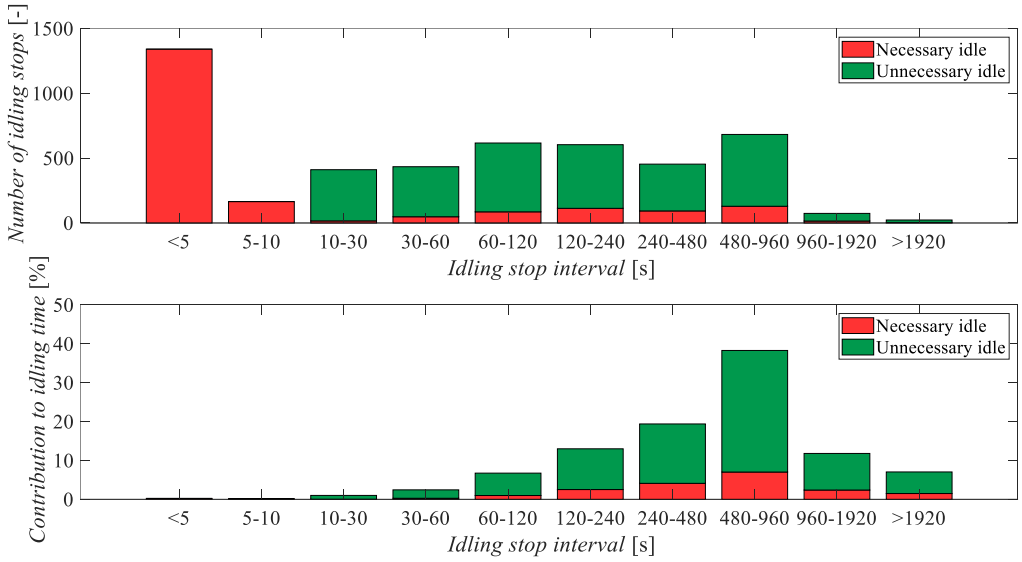

424

425 *Fig. 9 – In the graph at the top the number of stops at each idling stop time interval. In the*
426 *graph at the bottom is presented the definition of the percentage of influence of the*
427 *unnecessary idle and necessary idle over the total idle time.*

428 By definition of the unnecessary idling, all the idling stops shorter than 10 s were classified
429 as necessary. Most of the idling stops are shorter than 10 s (equivalent to 31% of the total
430 idling stops), however their contribution to the total idling time is negligible (less than 0.4%).
431 For idling stops longer than 10 s, unnecessary idling stops dominate necessary idling stops for

any time interval. For unnecessary idling, most of the contribution to the total idling time (i.e. 31.3%) and most of the idling stops (i.e. 554 stops) lies into the interval 480-960 s. Additionally, there are also a great number of idling stops in the time intervals 120-240 s (i.e. 531 stops) and 240-480s (i.e. 491 stops) but they respectively influence the total idling time by only 10.5% and 15.3% of the entire unnecessary idling (Fig 9, bottom).

In Table 4, the theoretical impact of the adoption of the SS system is reported.

Table 4 – Theoretical impact of the SS system on the tractor under study

f_{save} [l]	367.86
N° of engine start-ups imposed by the driver	1155
N° of additional engine start-ups caused by the SS system	2435
$m_{CO_2,save}$ [kg]	956.44
$m_{CO,save}$ [g]	21.26

For necessary and unnecessary idling statuses, the tractor consumed 449 L and 367.9 L of fuel, respectively. These are nearly 2% and 1.65% of the entire fuel consumption during the period of use of the tractor. The number of engine start-ups imposed by the driver during the period of use is 1155 (i.e., on average 4 engine start-ups per day). Adopting the SS system with the defined strategy, the number of engine start-ups will increase by 67%, leading to a much greater load on the starter and the battery, affecting their durability. Considering the additional engine start-ups (from tests results the average fuel consumption of a complete ignition is around 0.003 l) induced by the SS system, the potential fuel saving is 1.62% of the entire consumed fuel of the tractor. In contrast to the results obtained in (Whittal, 2012), where CO emissions increased for a diesel powered vehicle (BMW 118d) equipped with a SS system, this study indicates that CO emissions could be reduced with the use of a SS system in a tractor. Specifically, a 21.26 g CO reduction was calculated; unfortunately, a comparison with the total CO emissions cannot be done, as emissions were not monitored during the real

tests campaign due to the fact, the gas analyser could not be installed for a prolonged field experimentation. This could be explained by the fact that the idling stop distribution of on-road vehicles is different from the one of tractors, and in particular, tractors tend to be stopped for idling for longer than on-road vehicles.

4. Conclusions

Engine idling is a frequent operating status of agricultural tractors and it is mostly not necessary since the operator does not request any use of the three-point linkage or hydraulic remotes. Thus, the corresponding fuel and green-house emissions could be avoided and tractor manufacturers should address novel solutions to limit the engine idling. This paper reports the results of a feasibility study on the introduction of SS systems in agricultural tractors. To this goal, the energy required for engine start-up and the subsequent emissions were measured. In terms of fuel consumption and CO_2 emission, turning off the engine is recommended for stops longer than 4 s; while for CO emission, turning off the engine is recommended for stops longer than 134 s. Additional research is needed to evaluate the impact of different engines architectures (i.e., engine size, number of cylinders, etc.) on these figures. The potential fuel and emission savings reported in this study seem limited, but considering that only in the US there are 1.2 million tractors of the same power level of the tractor used in this study (USDA, 2019) and that these tractors can be used up to 850 hours per year (Mattetti et al., 2019), yearly reductions of 285.6million litres of fuel, and, respectively of 16.5 and 754 tons of CO and CO_2 emissions could be attained every year with tractors equipped with SS systems. These figures should be considered as first estimation of the impact of idling reduction on emission of agriculture mechanisation. The implementation of a SS dedicated to agricultural tractors requires some rework on the powertrain architecture.

In particular, more powerful and durable alternators are required for quickly recharging the battery in order to restore the energy required for start-ups and for enduring the much greater number of ignitions than those exposed by conventional tractors with no SS system (Ohmae et al., 2006). The ongoing electrification process of agricultural tractors will be an enabling technology for the introduction of SS systems in agricultural tractors. Moreover, with the electrification of the auxiliaries and hydraulic subsystem, there would be the possibility to run the auxiliaries also when the engine is off and this will permit to achieve greater savings than those reported in this study. Especially, since also the fuel and emissions for necessary idling could be eliminated, although they are lower than those of unnecessary idling. The advantage of SS systems is also in terms of comfort since farmers may carry out standing operations around the tractor with no engine noise and harmful gas emissions.

However, tractors with a sort of electrified devices are still under study and a few solutions have been proposed (Hahn, 2008; Troncon et al., 2019; Varani et al., 2021). Despite the potential benefits, these solutions will not reach the market within several years. In the meantime, researchers and disseminators must raise the farmers' awareness about the harmful effects and economic losses of unnecessary idling through proper dissemination activities.

Acknowledgements

This project was supported by PRIN (Research projects of significant national interest) notification 2017 "*Green SEED: Design of more-electric tractors for a more sustainable agriculture*", grant number: 2017SW5MRC.

References

Abas, M. A., Wan Salim, W. S.-I., Ismail, M. I., Rajoo, S., & Ricardo, M.-B. (2017). Fuel consumption evaluation of SI engine using start-stop technology. *Journal of Mechanical Engineering and Sciences*, *11*, 2967–2978. https://doi.org/10.15282/jmes.11.4.2017.1.0267

Argonne National Laboratory. (2015). *Long-Haul Truck Idling Burns Up Profits* (DOE/CHO-AC02-06CH11357-1503 7148).

ASTM International. (2011). *Standard Test Method for Determination of Nitrogen Oxides, Carbon Monoxide, and Oxygen Concentrations in Emissions from Natural Gas-Fired Reciprocating Engines, Combustion Turbines, Boilers, and Process Heaters Using Portable Analyzers* (ASTM D6522). www.astm.org

Brodrick, C.-J., Dwyer, H. A., Farshchi, M., Harris, D. B., & King, F. G. (2002). Effects of Engine Speed and Accessory Load on Idling Emissions from Heavy-Duty Diesel Truck Engines. *Journal of the Air & Waste Management Association*, *52*(9), 1026–1031. https://doi.org/10.1080/10473289.2002.10470838

Brodrick, C.-J., Lipman, T. E., Farshchi, M., Lutsey, N. P., Dwyer, H. A., Sperling, D., Gouse, I., S. William, Harris, D. B., & King, F. G. (2002). Evaluation of fuel cell auxiliary power units for heavy-duty diesel trucks. *Transportation Research Part D: Transport and Environment*, *7*(4), 303–315. https://doi.org/10.1016/S1361-9209(01)00026-8

BSI Standards. (2012a). *Specification for portable electrical apparatus designed to measure combustion flue gas parameters of heating appliances. General requirements and test methods* (N. 50379–1).

BSI Standards. (2012b). *Specification for portable electrical apparatus designed to measure combustion flue gas parameters of heating appliances. Performance requirements for apparatus used in statutory inspections and assessment* (N. 50379–2).

Gaines, L., Rask, E., & Keller, G. (2013). *Which Is Greener: Idle, or Stop and Restart?* Argonne National Laboratory. https://www.afdc.energy.gov/uploads/publication/which_is_greener.pdf

Ganesan, A., & Sundaram, S. (2012). *A Heuristic Algorithm for Determining State of Charge of a Lead Acid Battery for Small Engine Applications* (SAE Technical Paper N. 2012-32–0082). SAE International. https://doi.org/10.4271/2012-32-0082

Geerlings, H., & van Duin, R. (2011). A new method for assessing CO2-emissions from container terminals: A promising approach applied in Rotterdam. *Journal of Cleaner Production*, *19*(6), 657–666. https://doi.org/10.1016/j.jclepro.2010.10.012

Hadavi, S., Andrews, G. E., Li, H., Przybyla, G., & Vazirian, M. (2013). *Diesel Cold Start into Congested Real World Traffic: Comparison of Diesel and B100 for Ozone Forming Potential* (SAE Technical Paper N. 2013-01–1145). SAE International. https://doi.org/10.4271/2013-01-1145

Hahn, K. (2008). High Voltage Electric Tractor-Implement Interface. *SAE International Journal of Commercial Vehicles*, *1*(1), 383–391. https://doi.org/10.4271/2008-01-2660

International Council on Clean Transportation. (2016). *European Stage V non-road emission standards*. WWW.THEICCT.ORG

IPPC. (2014). *AR5 Climate Change 2014: Mitigation of Climate Change*. Cambridge University Press. https://www.ipcc.ch/report/ar5/wg3/

Kulikov, I., & Karpukhin, K. (2018). *Model Analysis of Efficiency and Energy Distribution in the Powertrain of an Electric Vehicle Equipped with a Solar Cell Battery* (SAE Technical Paper N. 2018-01–5026). SAE International. https://doi.org/10.4271/2018-01-5026

Lee, S., Fulper, C., McDonald, J., & Olechiw, M. (2019). *Real-World Emission Modeling and Validations Using PEMS and GPS Vehicle Data* (SAE Technical Paper N. 2019-01–0757). SAE International. https://doi.org/10.4271/2019-01-0757

Mattetti, M., Maraldi, M., Lenzini, N., Fiorati, S., Sereni, E., & Molari, G. (2021). Outlining the mission profile of agricultural tractors through CAN-BUS data analytics. *Computers and Electronics in Agriculture*, *184*, 106078. https://doi.org/10.1016/j.compag.2021.106078

Mattetti, M., Maraldi, M., Sedoni, E., & Molari, G. (2019). Optimal criteria for durability test of stepped transmissions of agricultural tractors. *Biosystems Engineering*, *178*, 145–155. https://doi.org/10.1016/j.biosystemseng.2018.11.014

Molari, G., Mattetti, M., Lenzini, N., & Fiorati, S. (2019). An updated methodology to analyse the idling of agricultural tractors. *Biosystems Engineering*, *187*, 160–170. https://doi.org/10.1016/j.biosystemseng.2019.09.001

Molari, G., Mattetti, M., Perozzi, D., & Sereni, E. (2013). Monitoring of the tractor working parameters from the CAN-Bus. *AIIA 13*. Horizons in agricultural, forestry and biosystems engineering, Viterbo.

Nada, Y., Komatsubara, Y., Pham, T., Yoshii, F., & Kidoguchi, Y. (2015). Evaluation of NOx Production Rate in Diesel Combustion Based on Measurement of Time Histories of NOx Concentrations and Flame Temperature. *SAE International Journal of Engines*, *8*(1), 303–313.

Ohmae, T., Sawai, K., Shiomi, M., & Osumi, S. (2006). Advanced technologies in VRLA batteries for automotive applications. *Journal of Power Sources*, *154*(2), 523–529. https://doi.org/10.1016/j.jpowsour.2005.10.049

Parravicini, M., Barro, C., & Boulouchos, K. (2020). Compensation for the differences in LHV of diesel-OME blends by using injector nozzles with different number of holes: Emissions and combustion. *Fuel*, *259*, 116166. https://doi.org/10.1016/j.fuel.2019.116166

Patton, R., & Bennett, G. (2011). *High Efficiency Internal Combustion Stirling Engine Development* (SAE Technical Paper N. 2011-01–0410). SAE International. https://doi.org/10.4271/2011-01-0410

Perozzi, D., Mattetti, M., Molari, G., & Sereni, E. (2016). Methodology to analyse farm tractor idling time. *Biosystems Engineering*, *148*, 81–89. https://doi.org/10.1016/j.biosystemseng.2016.05.007

Qiao, H., Zheng, F., Jiang, H., & Dong, K. (2019). The greenhouse effect of the agriculture-economic growth-renewable energy nexus: Evidence from G20 countries. *Science of The Total Environment*, *671*, 722–731. https://doi.org/10.1016/j.scitotenv.2019.03.336

Rakha, H. A., Ahn, K., Moran, K., Saerens, B., & Bulck, E. V. den. (2011). Virginia Tech Comprehensive Power-Based Fuel Consumption Model: Model development and testing. *Transportation Research Part D: Transport and Environment*, *16*(7), 492–503. https://doi.org/10.1016/j.trd.2011.05.008

583 Rudder, K. D. (2012). Tier 4 High Efficiency SCR for Agricultural Applications. *SAE*
584 *International Journal of Commercial Vehicles*, *5*(1), 386–394.
585 https://doi.org/10.4271/2012-01-1087

586 Saetti, M., Mattetti, M., Varani, M., Lenzini, N., & Molari, G. (2021). On the power demands
587 of accessories on an agricultural tractor. *Biosystems Engineering*, *206*, 109–122.
588 https://doi.org/10.1016/j.biosystemseng.2021.03.015

589 Salmasi, F. R. (2007). Control Strategies for Hybrid Electric Vehicles: Evolution,
590 Classification, Comparison, and Future Trends. *IEEE Transactions on Vehicular*
591 *Technology*, *56*(5), 2393–2404. https://doi.org/10.1109/TVT.2007.899933

592 Scolaro, E., Beligoj, M., Estevez Perez, M., Alberti, L., Renzi, M., & Mattetti, M.
593 (Submitted). Electrification of Agricultural Machinery A Review. *Proceedings of IEEE*, 1–
594 18.

595 Thitipatanapong, S., Noomwongs, N., Thitipatanapong, R., & Chantranuwathana, S. (2013). *A*
596 *Comparison Study on Saving Fuel by Idle-Stop System in Bangkok Traffic Condition* (SAE
597 Technical Paper N. 2013-01–0069). SAE International. https://doi.org/10.4271/2013-01-
598 0069

599 Troncon, D., Alberti, L., & Mattetti, M. (2019). A Feasibility Study for Agriculture Tractors
600 Electrification: Duty Cycles Simulation and Consumption Comparison. *2019 IEEE*
601 *Transportation Electrification Conference and Expo (ITEC)*, 1–6.
602 https://doi.org/10.1109/ITEC.2019.8790502

603 US EPA. (1997). *Determination of Nitrogen Oxides, Carbon Monoxide, and Oxygen*
604 *Emissions from Natural Gas-Fired Engines, Boilers and Process Heaters Using Portable*
605 *Analyzers* (CTM-030).

606 US EPA. (1999). *Draft Method for the Determination of O2, CO, & (NO and NO2) for*
607 *Periodic Monitoring* (CTM-034).

608 USDA. (2019). *2017 Census of Agriculture: U.S. Summary and State Data* (AC-17-A-51).
609 USDA. https://www.nass.usda.gov/Publications/AgCensus/2017/index.php

610 Varani, M., Mattetti, M., & Molari, G. (2021). Performance Evaluation of Electrically Driven
611 Agricultural Implements Powered by an External Generator. *Agronomy*, *11*(8), 1447.
612 https://doi.org/10.3390/agronomy11081447

613 Whittal, I. (2012). *Off-Cycle Fuel Consumption Evaluation of Stop-Start Systems* (SAE
614 Technical Paper N. 2012-01–1601). SAE International. https://doi.org/10.4271/2012-01-
615 1601

616 Wishart, J., Shirk, M., Gray, T., & Fengler, N. (2012). *Quantifying the Effects of Idle-Stop*
617 *Systems on Fuel Economy in Light-Duty Passenger Vehicles*. 2012-01–0719.
618 https://doi.org/10.4271/2012-01-0719

619